

Liquid State Control of Chemical Reactions: Toward a Molecular Description

M. BEN-NUN AND R. D. LEVINE*

The Fritz Haber Research Center for Molecular Dynamics, The Hebrew University of Jerusalem, Jerusalem 91904, Israel, and Department of Chemistry and Biochemistry, University of California, Los Angeles, California 90024

Received December 7, 1993

The concept of a reaction coordinate along which a system evolves en route from reactants to products is central to our understanding of the elementary act of the chemical change. When there is a barrier along the reaction coordinate, it can act as a bottleneck to transition and thus determine the rate of the reaction. Hence the first aspects that one wants are the details of the barrier region: How high is the barrier, and how narrow is the passage leading to it? There can also be one or more hollows along the reaction coordinate, and these correspond to shorter or longer lived reaction intermediates, depending on the depth of these hollows. In solution, the liquid will hinder the approach motion of the reactants. The barrier crossing is then not necessarily the rate-determining step, and the observed net reaction rate will also reflect the rate of diffusion of the reactants. Just as the liquid can hinder the approach motion of the reactants, it can also impede the products as they separate. This is the traditional cage effect.¹ Computer simulations can examine what happens inside the cage and what factors govern its manifestation. An exhaustive review of such simulations has recently been prepared by Whitnell and Wilson.² Overall views³ have been given by Hynes,⁴ Shroeder and Troe,⁵ and Wolynes and Fleming.⁶

The accumulated understanding of gas-phase reaction dynamics⁷ and that of the structure and dynamics of pure liquids,⁸ supplemented with the available computer power, enables one to monitor simultaneously the motion of two reactants that are being continuously buffeted by a solvent. The output from these simulations is a complete description of the time evolution of all particles in the system. Our attitude is that the mechanical, so-called molecular dynamics approach is like a very detailed experiment that calls for an interpretation. The very complexity of such a detailed mechanical description makes it necessary to develop simple models to interpret the results. One possible reduced stochastic description is based on modeling the role of the solvent via the introduction of an additional, dissipative (i.e., friction-like) term to the characterization of the motion. It is generally agreed that the resulting, so-called Langevin equation, or generalized Langevin equation (GLE) for the case of a frictional term with "memory" of the previous history of

the system, correctly describes averaged physical properties.⁹⁻¹² In this Account we discuss an equivalent approach, but one which is cast in purely mechanical terms, in order to model, analyze, and predict the results of trajectory computations of bimolecular reactions in solution. The mechanical description that we use can be recast in frictional terms, yet we believe that, just as in the gas-phase problems, a simple mechanical picture is useful.

Another complementary description that avoids the complexity of the many-atom problem is based on the frequency domain. The frequency spectrum of a large isolated molecule embodies in it much knowledge about the intrinsic (harmonic and anharmonic) forces. The vibrational, rotational, and wagging motions will typically have different frequencies and thus will span different regions in the IR spectrum. In a similar manner, the many-body problem of a small reactive system immersed in a liquid may be studied using spectroscopic tools if one is willing to picture the solvent and solute as a "large molecule". In particular we will be interested in the reactive system frequency and the solvent-solute coupling frequency. The tools for computing the power spectrum from classical trajectories are available.¹³ By using the Fourier transform to go over from the time domain to the frequency domain, the uncertainty relation is inherently built in and the time-energy complementarity of quantum mechanics is satisfied. In our work we use the classical power spectrum to study and interpret the dynamics of bimolecular reactions in solution.

(1) Frank, J.; Rabinowitch, E. *Trans. Faraday Soc.* 1934, 30, 120.

(2) Whitnell, R. M.; Wilson, K. R. In *Reviews in Computational Chemistry*; Lipkowitz, K. B., Boyd, D. B., Eds.; VCH: New York, 1993; Vol. IV.

(3) Recent collections of articles include the following: Hanggi, P., Troe, J., Eds. *Ber. Bunsen-Ges. Phys. Chem.* 1991, 95 (3). Burshtein, A., Kivelson, D., Eds. *Chem. Phys.* 1991, 152 (1, 2). Pullman, B., Jortner, J., Levine, R. D., Eds. *Reaction Dynamics in Clusters and Condensed Phases*; Reidel: Dordrecht, 1993.

(4) Hynes, J. T. In *Theory of Chemical Reaction Dynamics*; Baer, M., Ed.; CRC Press: Boca Raton, FL, 1985; Vol. IV.

(5) Shroeder, J.; Troe, J. *Annu. Rev. Phys. Chem.* 1987, 38, 163.

(6) Fleming, G. R.; Wolynes, P. G. *Phys. Today* 1990, May, 36.

(7) Levine, R. D.; Bernstein, R. B. *Molecular Reaction Dynamics and Chemical Reactivity*; Oxford University Press: Oxford, 1987.

(8) Allen, M. P.; Tildesley, D. J. *Computer Simulations of Liquids*; Calderon Press: Oxford, 1987. van Gunsteren, W. F.; Berendsen, H. J. C. *Angew. Chem., Int. Ed. Engl.* 1990, 29, 992.

(9) Adelman, S. A. *Adv. Chem. Phys.* 1983, 53, 61. Adelman, S. A. *Rev. Chem. Intermed.* 1987, 8, 321.

(10) Nitzan, A. *Adv. Chem. Phys.* 1988, 70, 489.

(11) Harris, C. B.; Smith, D. E.; Russell, D. J. *Chem. Rev.* 1990, 90, 481.

(12) Chandler, D. *J. Phys.: Condens. Matter* 1990, 2, SA9. Robinson, G. W.; Singh, S.; Krishnan, R.; Zhu, S. B.; Lee, J. J. *Phys. Chem.* 1990, 94, 4.

(13) Noid, D. W.; Kosykowski, M. L.; Marcus, R. A. *Annu. Rev. Phys.* 1981, 32, 267.

Michal Ben-Nun is a Clore Foundation doctoral fellow at the Hebrew University of Jerusalem. Her research interests are described in this Account.

Raphael D. Levine is the Max Born Professor of Natural Philosophy at the Hebrew University and a professor of chemistry at the University of California, Los Angeles. He has a long-standing interest in the dynamics of chemical reactions. He is a member of the Israel Academy of Sciences and a Wolf Prize Laureate and has received a number of awards and honorary degrees. His earlier biography appears in *Acc. Chem. Res.* 1974, 7, 393.

We begin with the role of a weakly coupled solvent¹⁴ in activating the thermal reactants. We explain and show why the intervention by such a solvent is typically confined to the foothills of the barrier to reaction. We also find it worthwhile to distinguish between the mere caging of the reactants and the "classical" cage where the coupling to the solvent is strong enough to induce recrossings of the barrier,^{15,16} which thereby results in thermodynamic control. The quantitative discussion emphasizes the realistic magnitudes of the forces along the reaction coordinate and of the interaction with the solvent. An important technical tool is the use of the adiabatic approximation¹⁷ and the separation of time scales which is thereby implied. We probe the latter by computing the relevant power spectra.

We pay particular attention to the participation of the solvent in the motion along the reaction path. The distinction between kinetic and thermodynamic control is discussed with special reference to reactions with a high chemical barrier. Further insight is provided by a study of activationless reactions (such as the recombination of an ion pair) in which the solvent takes an active part and the destruction of "solvent-separated" ion pairs¹⁸ is a prerequisite for reaction. A critique examines the limitations of the discussion and the scope for further work.

Activated Processes

To discuss the role of the solvent in activating the reactants we begin by examining the energy profile along the reaction coordinate q . Figure 1 is an example for a typical symmetric $A + BA$ atom exchange reaction and as such exhibits two (general) features. One is the relative short range of interaction: There is a range L , where L is typically of the order of 1 Å, such that at $q = \pm L$ one is already at the foothills of the barrier. Thus the gas-phase interaction region is well localized.^{19,20} The second important feature is the curvature of the potential. We use the second derivative of the potential along q , $K(q)$, as a measure for the frequency of the motion. If the motion is bound, then its local harmonic frequency is $\omega^2(q) = K(q)/\mu$ where μ is the mass. However, even if the motion is unbound, $(-K(q)/\mu)^{1/2}$ locally determines the time scale of the motion. (Of course, in this case the motion is an unstable one.) Hence the magnitude of the curvature of the potential (scaled by the appropriate mass factor) tells us the *local* time scale of the motion. At the top of the barrier the magnitude of the unbound force constant is similar to

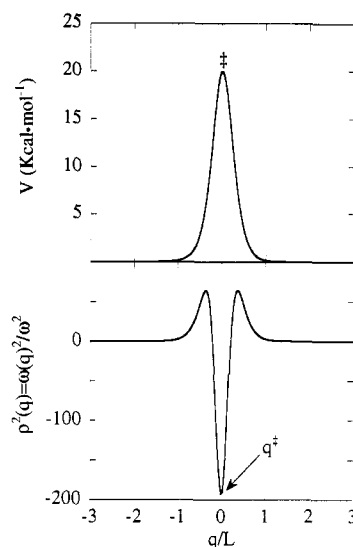


Figure 1. Upper panel: The general features of an energy profile along a reaction coordinate for a symmetric atom exchange reaction in the gas phase. Note that the gas-phase interaction potential has a short range, so that at $q = \pm L$ one is already at the distant foothills of the potential and $L \approx 1-2$ Å. Lower panel: The ratio of the (local) reaction coordinate frequency and the solvent-solute frequency ω , $\rho^2(q) \equiv \omega^2(q)/\omega_s^2$, vs the reaction coordinate q . (The mass μ in eq 1.1 and in the definition of $\rho^2(q)$ is that for the $\text{Cl} + \text{Cl}_2 \rightarrow \text{Cl}_2 + \text{Cl}$ atom exchange reaction.) At the barrier the motion is unbound, yet the magnitude of the curvature is a measure for the local time scale of the motion. It is the high value of the curvature at the barrier and the low value of ω in rare gas solvents that results in the solvent inability to interfere with the rapid barrier-crossing process.

that of a bound diatomic molecule, Figure 1. Thus the crossing of the barrier is a rapid event, with a typical duration of 10–50 fs.

A clear-cut "cage effect" (i.e., recrossings of the barrier) is seen in the simulations only at very high densities.²¹ Even then the details of the gas-phase potential are important, and many trajectories fail to recross the barrier if the steric and kinematic requirements, familiar from the gas phase, are not satisfied. As one increases the density (and thereby diminishes the mean and the variance of the intermolecular distances), a fairly abrupt onset of caging is evident at the same density at which self-caging of the solvent becomes important. During the very short barrier-crossing event one cannot really distinguish between a glassy phase and a liquid phase. A meaningful distinction between a glassy and a liquid state is possible only on much longer time scales. Rare gas glasses can therefore provide a useful medium for the experimental study of the dynamical role of the solvent in atom exchange reactions.

The simulations have further shown that the liquid is able to detain the reactants (and/or products) at the distant foothills of the barrier for long periods and that activation (or deactivation when looking at the descending products) is localized both in time and in position. An initial fluctuation²² that involves a few solvent atoms, adjacent to the reactants, provides the necessary energy to surmount the barrier (a few kilocalories/mole) via a few hard collisions that are localized in time (and in position). The activation

(14) Bergsma, J. P.; Reimer, J. R.; Wilson, K. R.; Hynes, J. T. *J. Chem. Phys.* **1986**, *85*, 5625. Benjamin, I.; Gertner, B. J.; Tang, N. J.; Wilson, K. R. *J. Am. Chem. Soc.* **1990**, *112*, 524.

(15) Kramers, H. A. *Physica* **1940**, *7*, 284.

(16) Recrossings of the barrier will reduce the magnitude of the reaction rate. For the computations of the latter, see: Grote, R. F.; Hynes, J. T. *J. Chem. Phys.* **1980**, *73*, 2715. Pollak, E. *Ibid.* **1986**, *85*, 865. Borkovec, M.; Berne, B. J.; Straub, J. E. *Ibid.* **1988**, *92*, 3711. Tucker, S. C.; Truhlar, D. G. *J. Am. Chem. Soc.* **1990**, *112*, 3347. Tucker, S. C.; Tuckerman, M. E.; Berne, B. J.; Pollak, E. *J. Chem. Phys.* **1991**, *95*, 5809. McRae, R. P.; Schenter, G. K.; Garrett, B. C.; Haynes, G. R.; Voth, G. A.; Schatz, G. C. *Ibid.* **1992**, *97*, 7392. Truhlar, D. G.; Schenter, G. K.; Garrett, B. C. *Ibid.* **1993**, *98*, 5756.

(17) Levine, R. D. *Quantum Mechanics of Molecular Rate Processes*; Oxford University Press: Oxford, 1969.

(18) Winstein, S.; Clippinger, E.; Fainber, A. H.; Robinson, G. C. *J. Am. Chem. Soc.* **1954**, *76*, 259. Ciccotti, G.; Ferrario, M.; Hynes, J. T.; Kapral, R. *J. Chem. Phys.* **1990**, *93*, 7137.

(19) Ben-Nun, M.; Levine, R. D. *J. Chem. Phys.* **1992**, *97*, 8341.

(20) Charutz, D. M.; Levine, R. D. *J. Chem. Phys.* **1993**, *98*, 1979.

(21) Ben-Nun, M.; Levine, R. D. *J. Phys. Chem.* **1992**, *96*, 1523.

(22) Wilson, K. R.; Levine, R. D. *Chem. Phys. Lett.* **1988**, *152*, 435.

process takes place a few hundreds of femtoseconds prior to the barrier crossing event, and it involves the creation of a "hot spot" in the liquid.

One should carefully note that we are talking about that subset of trajectories that do manage to scale the barrier. For a system initially in thermal equilibrium there is a much larger subset of nonreactive trajectories. To show that we can discuss only the subset of reactive trajectories, it is convenient to appeal to microscopic reversibility. In the present context this implies that any possible forward motion in time has an equally possible motion determined by propagating backward in time. Any trajectory that ascends to the barrier has as its counterpart a trajectory that descends from the barrier. This is a result that we will appeal to below. It also offers a rationalization of why it takes a few hard collisions to scale the barrier. Imagine a fast descent from a steep barrier. The descending species must at the foothills run into one or a few solvent atoms. In the next section we will make this description a shade more quantitative, but the essential point should be recognized already here: On the time scale of the descent from a typical chemical barrier, a weakly coupled solvent does not respond fast enough. The same considerations of microscopic reversibility also identify the subgroup of those trajectories that start as thermal separated reactants and do cross the barrier as the entire set of trajectories that begins at the barrier and, when propagated backward in time, descends into the reactants region.

It may be useful to recast our mechanical description using the concept of friction.¹⁵ For a friction which has no memory (what is known as the ordinary Langevin equation), the dissipation corresponds to many frequent but small random kicks, as one expects in a Brownian motion. The picture we have outlined is that of one or a few large kicks localized in time or, equivalently, in frequency. As discussed above, the reaction path frequency rapidly varies along the reaction coordinate so that the coupling to the solvent is localized in space. Using a generalized Langevin equation, where the friction is time dependent one can, in principle, mimic this localized coupling.

A Model of Activated Barrier Crossing in Solution. To understand the nature of the activation process, a reduced description of the many-body problem is useful. The minimal Hamiltonian needed to describe an atom exchange reaction in a liquid must account for the role of the solvent. We therefore introduce a two-dimensional model Hamiltonian that involves a motion along the reaction coordinate q which is linearly coupled to a harmonic solvent-solute coordinate r :

$$H = \left(\frac{m}{2}\right)\dot{r}^2 + \left(\frac{\mu}{2}\right)\dot{q}^2 + E(q) + \frac{k}{2}\left(r - \frac{C}{k}(q - q^*)\right)^2 \quad (1.1)$$

k is the harmonic solvent-solute force constant, $E(q)$ is the potential along the reaction coordinate, and q^* is the barrier's position. The linear coupling term C is related to the friction coefficient γ , which governs the overall rate of momentum dissipation in the Langevin equation. We use the simulations to determine the force constants via the relevant dominant frequencies in the power spectrum. The two masses m and μ are important in determining the dynamics. This model

considers only the motion along the reaction coordinate and neglects the other degrees of freedom of the transition state of the reactants. The role of these coordinates in the liquid is still an open question.

Before proceeding to describe the results, we define reduced parameters that can be derived¹⁹ from the equations of motion for the Hamiltonian (1.1). These reduced parameters govern the different possible modes of behavior and are measured in units of the solvent-solute frequency, ω , and its mass m . There are two: One is a reduced coupling constant,

$$\gamma^* \equiv (\gamma/\omega) = (C/k)^2(m/\mu) \quad (1.2)$$

which measures how promptly the solvent can respond to its coupling to the solute. The higher is ω , the faster can the solvent adjust to the motion of the reactants along the reaction coordinate. Therefore the raw strength of the coupling, γ , and the frequency, ω , scale one another. In the weak coupling limit (which is appropriate for rare gas solvents), $\gamma^* < 1$, and vice versa for strongly coupled solvents, such as protic ones capable of creating hydrogen bonds. The other frequency in our problem is that for the motion along the reaction coordinate. An essential point is that this frequency is very different at different locations (at or about the barrier). Hence we use a reduced local frequency along the reaction coordinate:

$$\rho^2(q) \equiv \omega^2(q)/\omega^2 = (K(q)/k)(m/\mu) \quad (1.3)$$

$\rho^2(q)$ is the ratio between the reaction coordinate frequency and the solvent-solute frequency. As we shall argue, it is the high value of $|\rho^2(q)|$ for q at or about the barrier top (i.e., for $-L < q < +L$, where $|\rho^2(q)| \gg 1$) which accounts for the failure of rare gas solvents to effectively cage the reactants in the barrier region. Note, however, that eq 1.3 includes a mass factor, and therefore the disparity in force constants in the barrier region can be partially compensated by a light solvent and/or a heavy solute.

Below we discuss the adiabatic separation. We will take the adiabatic limit to be the one where the solvent is moving fast and is able to follow the motion along the reaction coordinate. The opposite is true in the sudden limit, where we have a fast motion along the reaction coordinate and a sluggish one along the solvent-solute mode. In both limits the solute can be strongly or weakly coupled to the solvent.²³

Adiabatic Separation. The disparity in the frequencies of the solvent motion and the motion along the reaction coordinate suggests that we introduce an adiabatic separation of coordinates. This is the exact analog of the Born-Oppenheimer approximation, with the fast motion corresponding to the motion of the electrons. This fast motion is able to adjust at every point in time to the instantaneous positions of the slow(er) coordinate(s). There are two important points of difference. First, it is only near the barrier top that the motion along the reaction coordinate is faster than the motion of the solvent. This is no longer true at the foothills of the barrier, so that nonadiabatic transitions will be important, and below we discuss them explicitly. The second is an important family of reactions for which the opposite is true, namely, that in the region of the

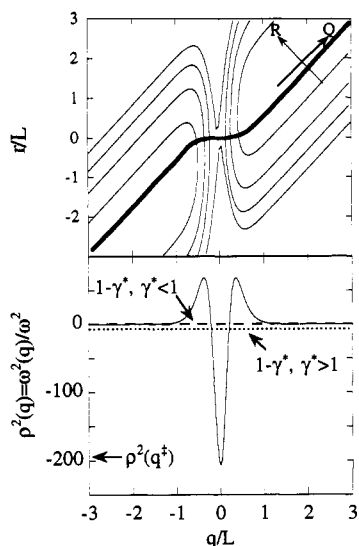


Figure 2. Upper panel: Contour plots of the two-dimensional model potential energy surface for a symmetric atom exchange reaction. The reaction coordinate is shown as a thick line. The equipotential contours are 1.5 kcal mol⁻¹ apart. Note the short range of the barrier region. The rotation angle θ is defined as the local tilt of the reaction coordinate Q with respect to the q axis where q is the reaction coordinate in the gas phase. Therefore Q corresponds to a concerted motion of both the solute and the solvent. The larger is θ , the more is the solvent mode participating in the motion along the reaction path Q . Note that θ is constant asymptotically and at the barrier. (The asymptotic value of θ is not 0 because the reactants/products are solvated.) Rapid changes in θ occur at the foothills on either side of the barrier to reaction. In passing through such a region the motion in the two adiabatic coordinates Q and R is no longer uncoupled. One can determine analytically that θ varies most with q at the point where $\rho^2(q) + \gamma^* = 1$. The bottom panel shows where this localized breakdown of the adiabatic separation takes place, for the weak ($\gamma^* < 1$) and strong ($\gamma^* > 1$) coupling regimes.

barrier to reaction it is the solvent motion which is faster. One characteristic of this family is the strong solvation of the reactants (which is absent in weakly coupled solvents, such as the rare gases).

The adiabatic procedure is based on a local harmonic approximation for estimating the time scale of the motion along the reaction coordinate. An adiabatic separation of variables is possible when one can neglect the local anharmonicity of the reaction coordinate potential. This enables us to diagonalize the coupling between the r and q motions via rotation of the coordinates by an angle θ ; see Figure 2. The "old" diabatic coordinate set is replaced by a new, adiabatic set, and the Hamiltonian is written as a sum of uncoupled terms. One new coordinate is that of crossing the barrier in the presence of the solvent. It is identified by being an unstable motion at the barrier top. Motion along this coordinate corresponds to a concerted motion of both the solute and the solvent. The other coordinate, orthogonal to the first one, represents the solvation mode. It too is a concerted motion of both solvent and solute and corresponds to the stable mode. The local frequency depends on q , and hence so does the rotation angle θ . As the system moves toward the barrier, θ changes, or in physical terms, the extent of solvent participation in the reaction path changes. If this change is too rapid, the adiabatic separations will break down.

The efficiency of energy transfer is related to the adiabaticity parameter, ξ . The motion is adiabatic if

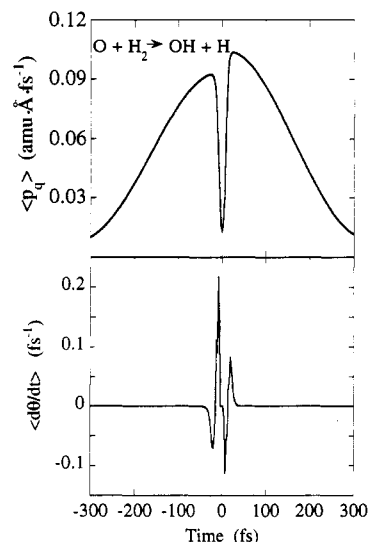


Figure 3. The momentum and the nonadiabatic coupling $d\theta/dt$ (on either side of the barrier) vs time. The value of the reduced friction, $\gamma^* = 0.7$, is realistic for reactions in fluid Ar at a density of 1.4 g mol⁻¹ at 300 K. All trajectories are initiated at $t = 0$ from the top of the barrier with a thermal distribution in all other degrees of freedom. The motion gains momentum, due to the descent from the barrier, up to the crossing point (where $d\theta/dt$ is extremal). The nonadiabatic transition converts most of the barrier energy to the r motion.

($d\theta/dt$) is small compared to the frequency ω of the r motion; i.e., when $\xi > 1$, $\xi = (\omega/(d\theta/dt))$. In the nonadiabatic limit the angle is changing rapidly, $\xi < 1$, and the impulsive deactivation (or activation) process is efficient.

The minimum energy path for a model reaction is shown in the upper panel of Figure 2. During most of the motion the adiabatic rotation angle is constant, and only to the right and to the left of the ridge is it changing rapidly. It is at these "dangerous" regions, where the surface is curving, that the solvent-solute motion will couple to the reaction coordinate via a resonant local frequency matching that is shown in the lower panel of Figure 2. Other than that, the motion is in the weak coupling limit, and the separation of variables is de facto exact. The molecular dynamics (MD) simulations discerned this local frequency matching via a large and fairly impulsive energy transfer from the solvent to the solute as the latter is ascending the barrier. Note that using time reversibility arguments one can equally well view this as an energy transfer from the solute to the solvent as the former is rapidly descending from the barrier and is abruptly brought to a halt by the surrounding solvent. The same phenomenon was observed in the model Hamiltonian and is shown for an ensemble of model trajectories in Figure 3. The motion down (or to) the barrier is essentially unperturbed, and the products (or reactants) gain (or lose) all the available energy. Only when the foothills of the barrier are reached a vibrational nonadiabatic impulsive energy transition deactivates (activates) the products (reactants). For physical values of the friction term these nonadiabatic transitions are confined to the foothills of the barrier. Note that even though the results are for an ensemble of 500 trajectories, they all undergo activation (deactivation) at a similar time following the departure of the barrier at $t = 0$. Until this localized transition, the solvent is practically frozen during the rapid barrier descent.

Typical atom exchange reactions have a barrier with a rather short range, and the curvature of the potential is therefore quite high. It requires a very special solvent, with special properties, to be able to rapidly respond to this fast motion. Quantitatively, the local ratio of the frequencies along the reaction coordinate and the solvent-solute motion is a measure for that. In the fast solvent response regime, $|\rho^2(q)| \leq 1$, but this only happens at the foothills of the potential. In the barrier region $|\rho^2(q)|$ is high, and the solvent is frozen and unable to follow the solute motion.²³ This was observed even for model S_N2 reactions in water.²⁴

Solvation. The adiabatic separation of variables determines, quantitatively, the extent of which the solvent contributes to the motion along the actual reaction path. In the region of kinetic control there is a limited solvent contribution to the motion across the barrier. This is typically the case in nonpolar solvents and/or in reactions with above thermal barrier heights. In the opposite extreme, the solvent responds much faster than the solute. The solvent control is then thermodynamic in that the solvent is in equilibrium with every configuration of the solute, and it induces recrossings of the barrier. We reiterate that simulations and our model considerations suggest that for many realistic cases one is in the region of kinetic control. Such will not necessarily be the case for reactions of ions in highly polar solvents.^{23,24}

Caging. When collisions of reactants with the solvent first solvation shell reverse the sign of their momentum, the particles remount the potential barrier, and they may even pass again through the crossing point. In agreement with the MD results, caging takes place only at such high densities that the friction (or, in our mechanical terms, coupling) is much higher (Figure 4). Under such circumstances the system cannot move unimpeded between two solvent molecules. When this is the case, the trajectory can recross the transition state, and every recrossing is accompanied by a nonadiabatic impulsive energy transfer at either side of the barrier. In these transitions energy is transferred out of or into the motion along the adiabatic reaction path. When the value of the friction is high, i.e., $\gamma^* > 1$, these transitions can take place closer to the barrier region, where the curvature is still negative, i.e., $\rho^2(q) < 0$. Not every reflected trajectory must successfully recross the barrier. The reactant motion along the barrier is fast, and the solvent may not reorganize to facilitate the recrossing of the barrier. When the solvent does not have the time to adjust and reoptimize the transition-state configuration, the trajectories which are caged at the foothills of the barrier and are reactivated are then reflected from the top of the barrier. In the adiabatic limit the solvent-solute motion is able to follow the motion along the reaction coordinate, i.e., the r and q motions are synchronized. An unfavorable configuration of the transition state is a diabatic effect, and it reflects a nonequilibrium configuration of the transition state.

Separation of Time Scales. The separation of time scales is due to a large difference in the magnitude of the reduced parameters for the different locations along

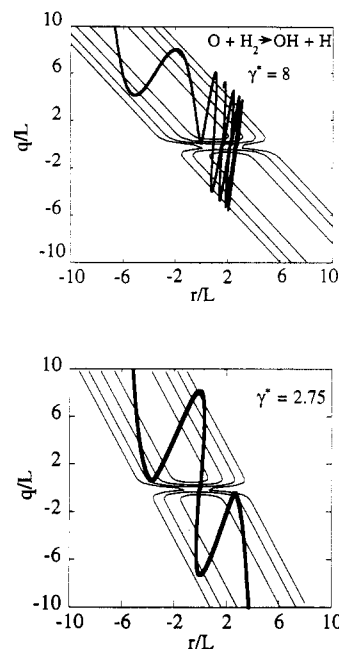


Figure 4. Upper panel: A model trajectory superposed on the potential energy surface at a high value of the reduced friction. The repeated crossings of the barrier are due to a strong nonadiabatic $q-r$ energy exchange (not shown) any time the q motion approaches the barrier. At lower values of γ^* (lower panel), the solvent fails to track the motion along the reaction coordinate and the recrossing attempts fail. Note the larger value of the rotation angle θ for stronger solvation.

the reaction coordinate. The different time domains can be discerned in both the molecular dynamics simulations and the reduced model and are conveniently explored in the frequency domain. Here we consider but one example, that of the “cage” motion.

Collisions with the liquid atoms can detain the products (and/or reactants) at the distant foothills of the activation barrier. These repeated collisions with the rare gas atoms (lower panel of Figure 5) generate a “collision-induced” spectrum in the far IR region.²⁵ We refer to these collisions as a “caged” motion as they confine the reactants to the region of chemical forces. In other words, we make a distinction between the classical “cage effect”, in which the reactants (or products) are made to retrace their descent and rescale the barrier, and the more general notion of a caged motion. The upper panel of Figure 5 shows this distinct frequency of the solvent-solute motion.

Activationless Processes

As in the gas phase, two classes of reactions, activated and activationless, serve as opposite models for simple bimolecular reactions. The first category will typically involve a reaction between neutral atoms or molecules whereas the second category includes radical recombination, ion-molecule reactions, and exchange reactions between polar reactants.^{18,24,26,27} Typical of such reactions is a long-range attraction exemplified in ion-molecule reactions by a well due to the ion-molecule polarization forces. Closer in, there may also be a barrier

(25) Ben-Nun, M.; Levine, R. D. *J. Phys. Chem.* 1993, 97, 2334.

(26) Straub, J. E.; Berne, B. J. *J. Chem. Phys.* 1988, 89, 4833. Keirstead, W. P.; Wilson, K. R.; Hynes, J. T. *Ibid.* 1991, 95, 5256.

(27) Ben-Amotz, D.; Harris, C. B. *J. Chem. Phys.* 1987, 86, 5433. Bagchi, B.; Fleming, G. R. *J. Phys. Chem.* 1990, 94, 9.

(24) Bergsma, J. P.; Gertner, B. J.; Wilson, K. R.; Hynes, J. T. *J. Chem. Phys.* 1987, 86, 1356. Gertner, B. J.; Whitnell, R. M.; Wilson, K. R.; Hynes, J. T. *J. Am. Chem. Soc.* 1991, 113, 74.

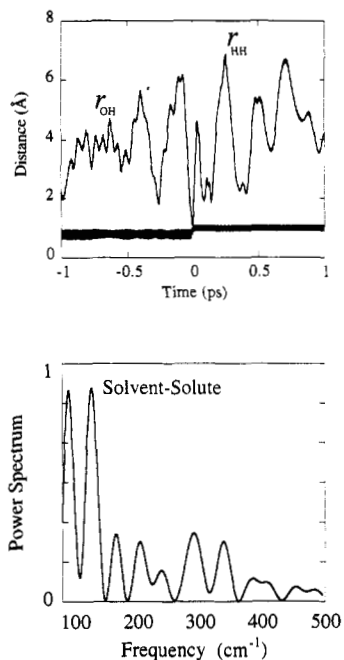


Figure 5. Upper panel: A molecular dynamics reactive trajectory for the $O + H_2 \rightarrow OH + H$ reaction in fluid Ar at a density of 1.4 g mol^{-1} and 300 K. The two bond distances are plotted vs time. We start with a bound H_2 molecule, the barrier is crossed (rapidly) once, and an OH product molecule is formed. The reactants (products) are determined for a long period within the first solvation shell, at the distant foothills of the chemical activation barrier, due to frequent collisions with the liquid. Lower panel: An averaged power spectrum of the solvent atom–solute atom motion vs frequency as determined from the full molecular dynamics. The frequent collisions with the liquid generate a collision-induced spectrum in the far-IR region.

before the reaction can proceed to completion. Our study is concerned only with the first stage, namely, the capture into the long-range well, as it occurs in solution.²⁸ We do not address the exit out of this well en route to products.

In the absence of an intrinsic barrier to recombination, the only barrier to capture, in the gas phase, is due to the rotational motion of the approaching reactants. (The recombination of two methyl radicals is but one example of a reaction with a rotational barrier.) The position of this rotational barrier is at a large separation (when measured in units of the interaction length scale). There are two, unrelated, different reasons why the activationless process is so different from the previous problem: (1) the reactants' long-range interaction is physical and is therefore weaker compared to a chemical interaction, and (2) the interaction with the solvent is different. We have an ion or a polar reactant which at room temperature is typically bound to one (or more) liquid atoms, and the two are vibrating around their equilibrium distance. In and about the rotational barrier region the solvent is moving faster than the slowly diffusing reactants (in our notation this is noted by $\rho^2(q) < 1$). Only to the left of the rotational barrier, i.e., near the equilibrium distance, do the reactants feel a strong chemical attraction. This disparity in forces governs the different major aspects of the recombination dynamics.

Molecular dynamics trajectories of a model ion–structureless molecule recombination in an atomic

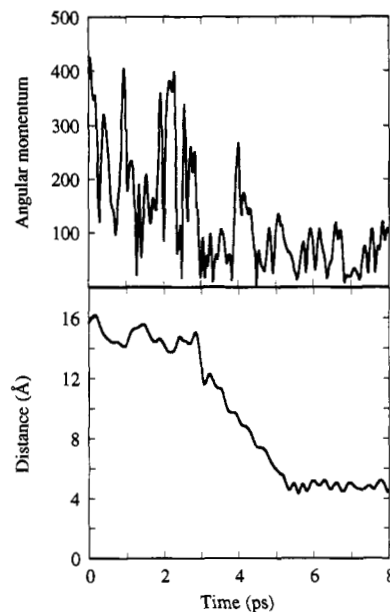


Figure 6. A typical molecular dynamics trajectory for the activationless recombination of an ion and a structureless molecule in liquid Ar. Lower panel: The relative ion (modeled as Cl^-)–molecule (modeled as a CH_3Cl “atom”) distance vs time in picoseconds. Note the capture (due to efficient stabilization of the ion pair by the solvent) at longer periods. Upper panel: The angular momentum j (in units of \hbar) of the ion–“molecule” relative separation as a function of time. In the gas phase, the simple capture model assumes that j is constant during the crossing of the centrifugal barrier. Here j is changing rapidly due to the buffeting of the reactants by the solvent.

solvent show this strong ion–solvent relative interaction. In contrast to the gas-phase problem where the ion–molecule rotational quantum number is constant, here it is changing rapidly and with a frequency that is similar to the ion–solvent vibrational frequency, Figure 6. This correlation may be checked by comparing the frequency of the Fourier transform of the ion–solvent distance (Figure 6, lower panel) to that of the ion–molecule rotational quantum number (Figure 6, upper panel).

The simulations have further pointed to the possible formation of a “solvent-separated” ion pair. At a large ion–molecule relative separation a solvent “atom” can fit in between the two reactants.¹⁸ The formation of an ion–molecule pair is then delayed, and it requires the reorganization of the solvent. As the ion–solvent separation decreases, two interactions are changing, and they both “push” the solvent to the other side of the ion: The ion–molecule *attraction* is increasing, and the molecule–solvent atom *repulsion* is increasing. Thus at a large ion–molecule distance the energetically stable configuration is ion–solvent–molecule, and as the ion–molecule separation continues to decrease the stable configuration is solvent–ion–molecule. Once it is formed the ion–molecule pair can be stabilized by collisions with the solvent. This sequence of events is shown in the lower panel of Figure 7. In the gas phase an attempted recombination process of two structureless reactants ends in their final ultimate separation, due to conservation of energy. One needs a chaperone or a third atom for stabilization of the adduct. The presence of the liquid provides this channel for energy dissipation, if energy transfer to the ion–solvent mode is efficient. Using an adiabatic separation of variables we identify the point in time that gives the major

(28) Ben-Nun, M.; Levine, R. D. *Chem. Phys. Lett.* **1993**, *214*, 175. Ben-Nun, M.; Levine, R. D. *J. Chem. Phys.* **1993**, *100*, 3594.

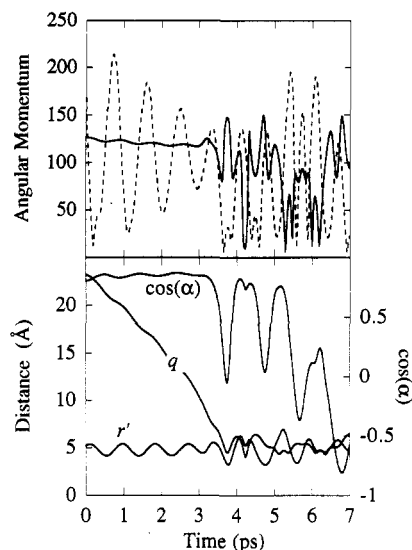


Figure 7. A trajectory for the activationless recombination reaction for the model. Lower panel: The ion-molecule separation, q , and the ion-solvent atom separation r' . α is the angle between the ion-molecule and the ion-solvent distances. At a large ion-molecule separation the stable configuration is molecule-solvent-ion ($\cos \alpha = 1$); as the relative separation decreases, the solvent rotates to the other side of the ion ($\cos \alpha = -1$) and an ion pair is formed. The efficient energy exchange (not shown) between the reaction coordinate and the solvation coordinate results in the formation of a stable adduct. Upper panel: The angular momentum j of the ion-molecule separation q (in units of \hbar) (dashed line) and the angular momentum in the adiabatic limit (solid line) vs time. During the barrier crossing, the separation of variables is de facto exact and the adiabatic angular momentum is constant whereas, in agreement with the full simulation (Figure 6), j is constantly changing. The constant value of the adiabatic angular momentum enables us to extend the gas-phase capture model to solution.

contribution to this energy transfer. The efficient energy transfer between the ion-molecule relative coordinate and the solvent-solute mode due to these vibrationally nonadiabatic transitions is confined to the ion-pair polarization well, and the approach motion itself is in the adiabatic limit. Thus the adiabatic separation enables us to use the gas-phase capture model, suitably modified to incorporate the dynamical role of the solvent motion, in solution. A motion along one uncoupled adiabatic coordinate describes the capture process. During the approach motion the angular momentum for this coordinate is constant (upper panel of Figure 7), and it thereby provides a quantitative criterion for capture. Qualitatively, what our discussion emphasizes is that a concerted motion of both the solvent and the solute modes takes place during the capture process. This is unlike the situation in weakly coupled solvents.

Critique

In the present Account only one stable frequency was assigned to the solvent, yet in a real solvent there is obviously a spread of frequencies. During the short time dynamics, the frequency spectrum of the liquid is not unlike that of a solid. There are, however, two important differences. Unlike the solid, the atoms (or molecules) of the liquid are not necessarily at or near the bottom of the potential. Hence the vibrational spectrum of a liquid can exhibit imaginary frequencies

that correspond to unstable motions.^{29,30} The second difference is the partial absence of long-range order. In this sense the liquid is at short times more similar to a glass. Furthermore, molecular liquids will have frequency bands corresponding to their internal motions. We consider that the spread of frequencies in the solvent, and the solvent internal modes, can further enhance the vibrational nonadiabatic deactivation (and/or activation) processes.

The use of one effective mode to describe the solvent interaction with the reaction coordinate is motivated by the evident separation of time scales. If we start with a Hamiltonian similar to eq 1.1 but with a large number of solvent harmonic oscillators (each with its own frequency), we can transform the problem to that of one effective solvent-solute mode that is coupled to the reaction coordinate. This mode is then coupled to a second solvent mode etc. Thus a hierarchy of successive interactions is generated. The solvent modes may be viewed as the different solvent shells around the solute, and the dissipation of energy is then perceived as a sequential event. Momentum is first dissipated to the first solvation shell, which will next dissipate it into the second shell and so on. For activated reactions the motion along the reaction coordinate is fast, and the secondary (and higher) interactions with the solvent are less important as they take place on a much longer time scale. In the activationless problem the higher interactions may be more important as the solvent and solute motions have a similar time scale.

In the full dynamics, the solute is coupled to all possible modes of the solvent. If we restrict our consideration to the solute motion along the reaction coordinate, the effective solvent-solute force constant k , eq 1.1, is given by

$$k = \sum_i \lambda_i^2 k_i / \sum_i \lambda_i^2 \quad (1.4)$$

This is in the form of a weighted average, with summation over all modes of the solvent. λ_i is the coupling strength of the i th mode of the solvent to the solute, and k_i is the force constant of the i th mode of the solvent. Equation 1.4 exhibits explicitly the role of the magnitude of the solvent frequencies and of the spread in these magnitudes on the value of k . The weighted averaging over the k_i 's shows that only such modes that simultaneously have higher frequencies and strong coupling to the solute contribute in an effective manner to k . In the same notation, C , the strength of the solvent-solute coupling defined in eq 1.2, is given by $C^2 = \sum_i \lambda_i^2$. Unlike k (or the mass m), the value of C^2 increases with the number of solvent modes with which the solute is effectively coupled.

In principle, the unstable modes of the rare gas solvent may provide the necessary mechanism for an efficient energy exchange between the solvent and the reaction coordinate when the latter is still in the barrier region. However, simulations of atom exchange reactions in rare gas solvents did not show this effect. The magnitude of the curvature of the chemical barrier was shown to be similar to that of a diatomic force constant. The unstable modes of a rare gas have longer time

(29) Stillinger, F. H.; Weber, T. A. *Science* 1984, 225, 983.

(30) Seeley, G.; Keyes, T. J. *J. Chem. Phys.* 1989, 91, 5581.

scales³⁰ and therefore cannot couple very well to this high-frequency motion. However, more associated solvents may have higher frequency unstable modes that can couple more effectively to the reaction coordinate in the chemical barrier region. Another higher frequency motion is that due to the internal vibrations of polyatomic solvents. These will be particularly coupled to the solute coordinates when they are infrared active.⁷

Concluding Remarks

In this Account we have discussed both the activated and the activationless dynamics of bimolecular reactions in structureless solvents. The role of the solvent during the motion to or from the barrier region, and in particular in the process of activating (or deactivating) the reactants, was analyzed via an adiabatic separation of variables. This not only identifies the nature of energy exchange between solvent and solute but also emphasizes the participation of the solvent motion in the chemical transformation of the solute.

Two extreme limits were discussed. The low coupling limit occurs where the solvent control is kinetic. Here the solvent couples to the solute primarily in the entrance or exit to the barrier region. This was interpreted in terms of the relevant frequencies (or force constants): the local frequency along the reaction coordinate and the solvent-solute frequency. The large repulsive forces at the activation barrier are often comparable to chemical force constants and are larger

by 1 or 2 orders of magnitude than the solvent-solute interaction. In the barrier's region the motion along the reaction coordinate is therefore fast whereas the solvent is moving slowly and is unable to follow this rapid motion. Only at the foothills of the activation barrier can the two local frequencies match, and an impulsive, nonadiabatic transition activates (deactivates) the reactants (products). The disparity in the magnitude of the force constants results in a separation of time scales that can be probed by spectroscopic means. For weakly coupled solvents, the caging regime is found only at such high densities that the solvent atoms themselves become caged. Even at these high densities the caging phenomenon is less pronounced than what one may expect, as the steric and kinematic requirements, familiar from the gas phase, must be satisfied for the recrossing of the barrier to be successful. The dynamics in strongly coupled solvents necessarily exhibit more variations reflecting chemical specificities. These are due not only to energetic effects but also to the dynamics which requires that during the chemical change there occurs a concerted motion of both solvent and solute.

We thank Prof. Gert van der Zwan for a critical reading of the manuscript and for his useful comments. This work was supported by the Air Force Office of Scientific Research. The Fritz Haber Research Center is supported by the MINERVA Gesellschaft für die Forschung, mbH, Munich, Germany.